

An analytical model based on the G -equation for the response of technically premixed flames to perturbations of equivalence ratio

Alp Albayrak and Wolfgang Polifke

Abstract

A model for the response of technically premixed flames to equivalence ratio perturbations is proposed. The formulation, which is an extension of an analytical flame tracking model based on the linearized G -equation, considers the flame impulse response to a local, impulsive, infinitesimal perturbation that is transported by convection from the flame base towards the flame surface. It is shown that the contributions of laminar flame speed and heat of reaction to the impulse response exhibit a local behavior, i.e. the flame responds at the moment when and at the location where the equivalence ratio perturbation reaches the flame surface. The time lag of this process is related to a convective time scale, which corresponds to the convective transport of fuel from the base of the flame to the flame surface. On the contrary, the flame surface area contribution exhibits a non-local behavior: albeit fluctuations of the flame shape are generated locally due to a distortion of the kinematic balance between flame speed and the flow velocity, the resulting wrinkles in flame shape are then transported by convection towards the flame tip with the restorative time scale. The impact of radial non-uniformity in equivalence ratio perturbations on the flame impulse response is demonstrated by comparing the impulse responses for uniform and parabolic radial profiles. Considerable deviation in the phase of the flame transfer function, which is important for thermo-acoustic stability, is observed.

Keywords

Equivalence ratio perturbation, flame dynamics, flame transfer function, impulse response, technically premixed flames

Date received: 11 June 2017; accepted: 11 October 2017

1. Introduction

Lean fuel–air mixtures allow low-emission combustion processes in a variety of industrial applications. However, operating under such conditions increases the chance of thermo-acoustic instabilities. In order to analyze, predict and control instabilities that result from flow–flame–acoustic interactions, the dynamic response of flames to perturbations is an active research topic. Premixed flames are sensitive to perturbations of upstream velocity as well as equivalence ratio.^{1,2} The present study focuses on the latter response mechanism.

The so-called G -equation—a level set equation³—has been used in a variety of studies on the response of a premixed flame to velocity perturbations.^{4–6} To the authors' knowledge, Dowling and Hubbard⁷ were the

first to propose a model based on the G -equation for the response to equivalence ratio perturbation. In the framework of that model, Lieuwen and co-authors^{8,9} identified three major contributions to perturbations of flame heat release as heat of reaction, laminar flame speed, and flame surface area; and provided an analytical expression for the flame transfer function (FTF) by solving the linearized G -equation in the frequency domain. An equivalent time-domain formulation, which yields the flame impulse response (IR)

Faculty of Mechanical Engineering, Technical University of Munich, Garching, Germany

Corresponding author:

Alp Albayrak, Thermo-Fluid Dynamics Group, Technical University of Munich, Boltzmannstr. 15, D-85748 Garching, Germany.
Email: albayrak@tfd.mw.tum.de



rather than the frequency response, was proposed by Albayrak et al.¹⁰ This approach explicitly reveals two global time scales of the flame response, related to the propagation of the perturbation along the flame surface and the restoration of flame shape. These time scales were identified previously in the flame response to velocity fluctuations, as explained in detail by Blumenthal et al.¹¹

All the models cited in the previous paragraph assume perturbations of equivalence ratio that are uniform across the mixing duct. This is a strong assumption, which will in general not be satisfied in practical applications with so-called technical premixed flames,^a where fuel–air mixing is not perfect, such that mean as well as fluctuations of equivalence ratio will exhibit some non-uniformity. The present study proposes an extended, time-domain-based analysis of the effect of perturbations of equivalence ratio on flame heat release rate, which relaxes this assumption. In particular, the flame IR to a local, impulsive, infinitesimal perturbation of fuel concentration is derived analytically. The approach allows to determine the flame response to any kind of equivalence ratio perturbation profile as a convolution over the local perturbations. Moreover, the infinitesimal perturbation gives insight to the flame response mechanisms: the direct contributions, i.e. the heat of reaction and laminar flame speed, are local processes with a convective time delay, whereas the flame surface area contribution exhibits a convective nature, which is triggered locally.

In the next section the derivation of the local IR is given for a laminar conical Bunsen flame. The IR that corresponds to an uniform perturbation profile¹⁰ is recovered, which validates the approach. Then, several perturbation profiles are investigated. It is shown that the perturbation profile has an impact on the phase of the FTF.

2. Model

The flame IR model is derived for a laminar, axisymmetric, conical flame (see Figure 1), which has been investigated repeatedly with analytical approaches.^{8–10} It is possible to formulate the model for other flame shapes, e.g. V- and M-shaped flames, however this is not explicated in this paper. The flame is subjected to an impulsive local equivalence ratio perturbation $\phi'_a(t, z, r)$ around infinitesimal vicinity of the radius a . This is illustrated in Figure 1 with a blue circle. This reads mathematically

$$\phi'_a(t, 0, r) = \bar{\phi} \delta(r - a) \delta(t) \quad (1)$$

where $\delta(t)$ is the Dirac delta function. Without essential loss of generality, the axial position of the perturbation

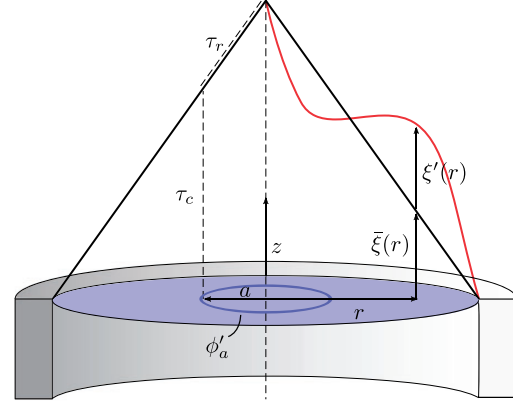


Figure 1. Illustration of the flame configuration. The mean and perturbed flame front are shown by black and red lines, respectively. Blue surface indicates the mean uniform equivalence ratio. The circle with radius a indicates infinitesimal hollow equivalence ratio perturbation. τ_c and τ_r indicate local time scales for propagation of the perturbation and restoration, respectively.

is assumed to be located in the flame base $z=0$. The corresponding IR in heat release rate $h_a(t)$ is defined implicitly by the relation

$$\frac{q'_a(t)}{\bar{q}} = \int_{-\infty}^{\infty} h_a(t - \tau) \frac{\phi'_a(t, 0, r)}{\bar{\phi}} d\tau \quad (2)$$

where q is the global heat release rate integrated over the whole flame.

2.1 Governing equations

To pursue analytical expressions the flow velocities are assumed to be uniform. The flame front kinematics is described by the level set method G -equation

$$\frac{\partial G}{\partial t} + \mathbf{u} \cdot \nabla G = s_L |\nabla G| \quad (3)$$

where s_L stands for the laminar flame speed.

The global heat release rate can be computed as

$$q = \int_f \rho s_L \Delta H dA \quad (4)$$

where ρ is density, ΔH is heat of reaction, and A is the flame surface area. The integral interval denoted by subscript “ f ” indicates that the integral is evaluated over the flame surface area. The flame surface area reads

$$A = \int_0^R 2\pi r \sqrt{1 + \left(\frac{\partial \xi}{\partial r}\right)^2} dr \quad (5)$$

The transport of mixture inhomogeneities can be modeled by the advection equation for the equivalence ratio. This mathematically reads

$$\frac{\partial \phi}{\partial t} + \mathbf{u} \cdot \nabla \phi = 0 \quad (6)$$

2.2 Modeled equations

Assuming small amplitude fluctuations, all equations described above are linearized. (\cdot) and $(\cdot)'$ indicate mean and fluctuating quantities, respectively. No velocity fluctuations are allowed, $\mathbf{u}' = 0$. It is assumed that the flame is surjective, i.e. $G(t, z, r) = z - \xi(t, r)$. The linearized ξ -equation reads

$$\frac{\partial \xi'}{\partial t} + c_r \frac{\partial \xi'}{\partial r} = -s'_L \sqrt{\left(\frac{\partial \bar{\xi}}{\partial r}\right)^2 + 1} \quad (7)$$

where c_r is the propagation speed in the radial direction of the flame restoration process (see Blumenthal et al.¹¹)

$$c_r = u_r + \frac{\bar{s}_L \frac{\partial \bar{\xi}}{\partial r}}{\sqrt{\left(\frac{\partial \bar{\xi}}{\partial r}\right)^2 + 1}} \quad (8)$$

The normalized and linearized heat release rate fluctuations q'/\bar{q} read

$$\frac{q'(t)}{\bar{q}} = \int_f \frac{\Delta H'}{\Delta \bar{H}} \frac{dA}{\bar{A}} + \int_f \frac{s'_L}{\bar{s}_L} \frac{dA}{\bar{A}} + \frac{A'}{\bar{A}} \quad (9)$$

where the density perturbations ρ' due to the equivalence ratio perturbations are assumed to be negligible. The impulsive perturbation simplifies the convolution integral in equation (2) and the IR can be explicitly defined as

$$h_a(t) \equiv \frac{q'_a(t)}{\bar{q}} = h_{\Delta H} + h_{s_L} + h_A \quad (10)$$

where three major contributions according to equation (9) are identified as heat of reaction $h_{\Delta H}$, laminar flame speed h_{s_L} and flame surface area h_A .

To calculate $h_{\Delta H}$ and h_{s_L} the fluctuating quantities, i.e. $\Delta H'$ and s'_L , should be modeled. This is done by first-order Taylor series expansion

$$\Delta H' = S_{\Delta H} \frac{\Delta \bar{H}}{\bar{\phi}} \phi' \quad (11a)$$

$$s'_L = S_{s_L} \frac{\bar{s}_L}{\bar{\phi}} \phi' \quad (11b)$$

where $S_{\Delta H}$ and S_{s_L} are defined as the respective sensitivities of the heat of reaction and the laminar flame speed to change in equivalence ratio

$$S_{\Delta H} \equiv \left. \frac{d\Delta H}{d\phi} \right|_{\phi=\bar{\phi}} \frac{\bar{\phi}}{\Delta \bar{H}} \quad (12a)$$

$$S_{s_L} \equiv \left. \frac{ds_L}{d\phi} \right|_{\phi=\bar{\phi}} \frac{\bar{\phi}}{\bar{s}_L} \quad (12b)$$

Following Abu-Off and Cant,¹² for a lean premixed methane air flame, the heat of reaction, and laminar flame speed are expressed as a function of equivalence ratio

$$s_L = A\phi^B e^{-C(\phi-D)^2} \quad (13)$$

$$\Delta H = \frac{2.9125 \cdot 10^6 \min(1, \phi)}{1 + 0.05825\phi} \quad (14)$$

where $A = 0.6079$, $B = -2.554$, $C = 7.31$, and $D = 1.23$. The flame surface area contribution h_A is calculated by the linearized flame surface area

$$\frac{A'}{\bar{A}} = \frac{\int_0^R 2\pi r \frac{\frac{\partial \bar{\xi}}{\partial r} \frac{\partial \xi'}{\partial r}}{\sqrt{\left(\frac{\partial \bar{\xi}}{\partial r}\right)^2 + 1}} dr}{\int_0^R 2\pi r \sqrt{1 + \left(\frac{\partial \bar{\xi}}{\partial r}\right)^2} dr} \quad (15)$$

The equivalence ratio perturbation $\phi'(t, z, r)$ is modeled by linearized advection equation

$$\frac{\partial \phi'}{\partial t} + u_z \frac{\partial \phi'}{\partial z} = 0 \quad (16)$$

3. Response of a conical flame

For a conical flame, the steady flame shape is expressed as

$$\bar{\xi}(r) = (R - r) \sqrt{\left(\frac{u_z}{\bar{s}_L}\right)^2 - 1} \quad (17)$$

and the flame restoration speed simplifies to

$$c_r = -\bar{s}_L \sqrt{1 - \left(\frac{\bar{s}_L}{u_z}\right)^2} \quad (18)$$

The solution of the ϕ' transport equation (16) with the boundary condition (1) reads

$$\phi'_a(t, z, r) = \bar{\phi} \delta(r - a) \delta\left(t - \frac{z}{u_z}\right) \quad (19)$$

Using equations (17), (18), and (19), the contributions to the IR can be expressed in closed forms. The following subsections provide the derivations for the heat of reaction and flame surface area contributions. The contribution of the laminar flame speed is analogous to that of the heat of reaction and therefore not discussed explicitly. Note that the derivations are valid for any equivalence ratio. For convenience, this paper presents only the results for lean flames with $\phi < 1$ and $S_{\Delta H} > 0$.

3.1 Heat of reaction contribution

The flame IR contribution of the heat of reaction is calculated by substituting the perturbation profile defined in equation (19) into equation (10)

$$h_{\Delta H}(a, t) = 2S_{\Delta H} \frac{a}{R^2} \delta(t - \tau_c) \quad (20)$$

where τ_c is the time scale related to the propagation of the equivalence ratio perturbation from the base to the flame surface which reads

$$\tau_c(a) = \frac{\bar{\xi}(a)}{u_z} \quad (21)$$

In Figure 1, the time scale τ_c is indicated as the dashed line, on which the equivalence ratio perturbation propagates. The IR is plotted in the left column of Figure 2 for five perturbation locations, i.e. $a = R \times [0, 0.25, 0.5, 0.75, 1]$. The IR is a local process. A positive impulsive response in heat release is observed at the instant when the perturbation reaches the flame surface. For $a = R$, the delay in the response is $\tau_c = 0$, since the perturbation acts immediately on the flame surface. The delay in the response increases as the location of the perturbation gets closer to the center. At the same time, the strength of the IR decreases. This is explained by the perimeter of the flame, which decreases with the radius. For the perturbation close to the center, the perturbation acts on a smaller perimeter and generates a weaker modulation of the overall heat release rate.

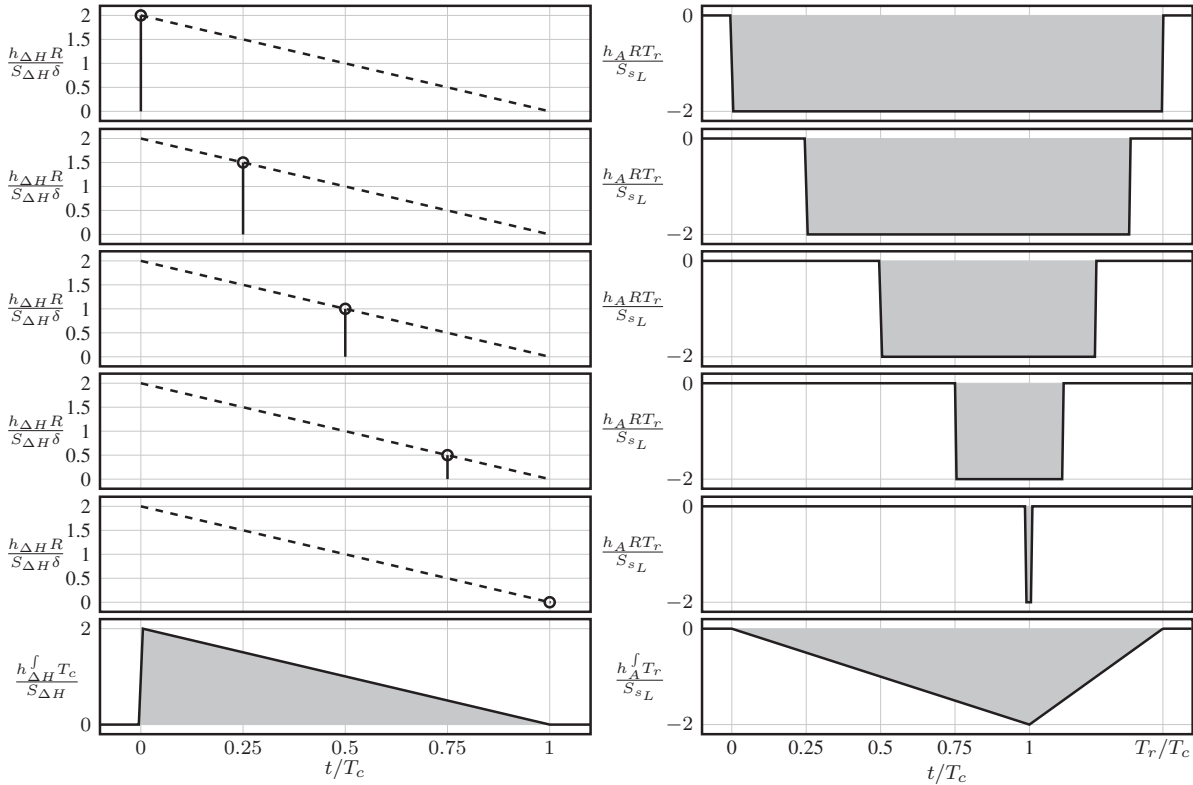


Figure 2. Heat of reaction (left) and flame surface area (right) contributions to the impulse response. From top to bottom, impulse responses with different perturbation locations are shown, respectively $a = R \times [1, 0.75, 0.5, 0.25, 0]$. Last row is the uniform impulse responses.

For validation purposes, the IR for a uniform equivalence ratio perturbation is obtained by integrating the local source over the radius, mathematically

$$h_{\Delta H}^f(t) = \int_0^R h_{\Delta H}(a, t) da \quad (22)$$

The final expression reads

$$h_{\Delta H}^f(t) = \frac{2S_{\Delta H}}{T_c^2} (T_c - t) [H(t) - H(t - T_c)] \quad (23)$$

where $T_c = \tau_c(0)$ is the convective time scale of the perturbation at the center. The detailed derivation is given in Appendix 1. This expression is the same as the one derived by Albayrak et al.¹⁰ The IR is plotted in last row on left column of Figure 2.

The same derivation also applies for the laminar flame speed contribution. Substituting ΔH with s_L in the equations in this subsection yields the IR for flame speed contribution.

3.2 Flame surface area contribution

First, the solution of equivalence ratio perturbation (equation (19)) is inserted to the linearized laminar flame speed (equation (11)). The resulting expression is then used as the right hand side term that is the source term for linearized ξ -equation (equation 7). The corresponding solution of the linearized ξ -equation reads

$$\xi_a'(t, r) = S_{s_L} \frac{u_z}{c_r} [H(r - a) - 1] \delta\left(t - \tau_c - \tau_r + \frac{r}{c_r}\right) \quad (24)$$

where $H(t) \equiv \begin{cases} 0, & t < 0 \\ 1, & t \geq 0 \end{cases}$ is the Heaviside step function, which is equal to the integral of the Dirac delta function

$$H(t) = \int_{-\infty}^t \delta(t') dt' \quad (25)$$

τ_r is the time scale of the restoration process and reads

$$\tau_r(a) = \frac{a}{c_r} \quad (26)$$

The time scale is illustrated in Figure 1 by the dashed line from the perturbed flame to the tip of the flame.

The flame surface area contribution defined in equation (10) is calculated via equation (15) and reads

$$h_A(a, t) = -2S_{s_L} \frac{c_r}{R^2} [H(t - \tau_c) - H(t - \tau_c - \tau_r)] \quad (27)$$

In right column of Figure 2, the IR contribution is plotted for different perturbation locations, i.e. $a = R \times [0, 0.25, 0.5, 0.75, 1]$. Contrary to the flame speed and heat of reaction contributions, the area contribution is not a local process. The contribution starts when the perturbation reaches with the flame, which is related with the convective time scale τ_c . Change in the laminar flame speed occurs at the location of contact and results in flame displacement. Assuming a lean premixed flame with positive equivalence ratio perturbation indicates that the flame displacement is in upstream direction and thus causes a negative response. This is shown in Figure 2. A negative response is generated at the time τ_c . Then, the perturbed flame is transported towards flame tip, which occurs with the restorative time scale τ_r . The IR contribution vanishes once the perturbed flame reaches the flame tip.

For validation purposes, the IR for uniform equivalence ratio perturbation is obtained by integrating the local source over the whole radius. Mathematically

$$h_A^f(t) = \int_0^R h_A(a, t) da \quad (28)$$

The final expression reads

$$h_A^f(t) = -\frac{2S_{s_L}}{T_c(T_r - T_c)} \times \left[\frac{T_c}{T_r} \{R(t - T_r) - R(t)\} - \{R(t - T_c) - R(t)\} \right] \quad (29)$$

where $T_r = \tau_r(R)$ is the global restorative time scale and $R(t) \equiv \max(t, 0)$ is the ramp function, which is equal to the integral of the Heaviside function

$$R(t) = \int_{-\infty}^t H(t') dt' \quad (30)$$

The IR is shown in last row of the right column of Figure 2. Again, this expression agrees with the results of Albayrak et al.¹⁰

4. Comparison of perturbation types

A generic description of the equivalence ratio perturbations can be defined as a boundary condition

$$\phi_a'(t, 0, r) = C_f(a) \bar{\phi} \delta(t) \quad (31)$$

The overall IR contribution h^f can be calculated from the local source IR h_a as

$$h^f(t) = \int_0^R C_f(a) h_a(t) da \quad (32)$$

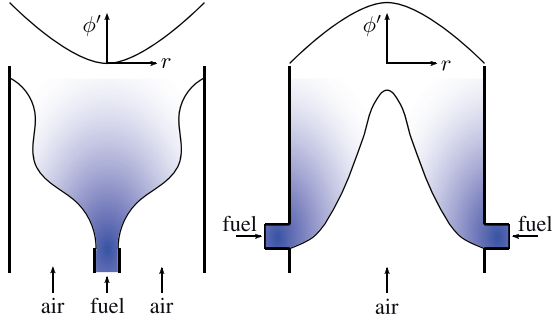


Figure 3. Sketches of two possible fuel injector configurations for technically premixed flames. Left: the fuel injection at the center and air supply as co-flow. Right: fuel supply from side walls. The blue color represents the equivalence ratio perturbations ϕ' . On top, ϕ' is plotted against the radius.

where C_f stands for the form factor, which is $C_f=1$ for the uniform perturbation.

For illustration purposes, an uniform perturbation profile is compared against parabolic profiles. Possible configurations are illustrated as sketch in Figure 3. In the left part of the figure, the choked fuel injection at the center with a co-flow air supply is shown. Flow perturbations in the air supply cause equivalence ratio fluctuations. The magnitude of the equivalence ratio perturbations is higher closer to the side walls, since the choked fuel flow prevents the penetration to the center region. In the right part of the figure, the reversed configuration is shown, i.e. the choked fuel injection is supplied through side walls. In this configuration, penetration to the side walls is prevented. This yields an equivalence ratio perturbation with higher magnitude in the center.

The form factors C_f^c and C_f^s indicate the case with center fuel injection and the side fuel injection, respectively. Perturbation strengths are kept constant as the uniform profile, i.e. $\int_0^R a C_f da = \int_0^R a da$. The form factors are approximated by parabolic functions

$$C_f^c = 2 \frac{a^2}{R^2} \quad (33)$$

$$C_f^s = 2 \left(1 - \frac{a}{R}\right) \left(1 + \frac{a}{R}\right) \quad (34)$$

The profiles are shown in Figure 4. The burner radius is $R=1$ mm, the axial flow velocity is $u_z=1$ m/s and the mean equivalence ratio is $\bar{\phi}=0.8$. Corresponding laminar flame speed is $\bar{s}_L=0.278$ m/s. The global convective time of perturbation is $T_c=3.45$ ms and the global restoration time scale is $T_r=3.74$ ms.

The IRs are shown in Figure 5. The solid line indicates the uniform perturbation profile, which also corresponds to the model derived by Albayrak et al.¹⁰ The

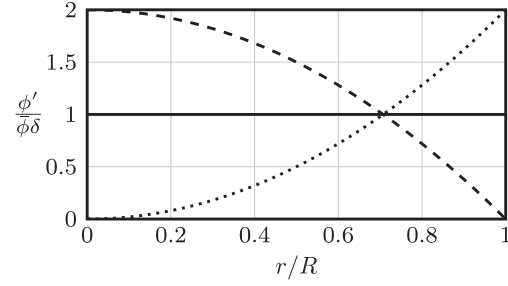


Figure 4. Different radial profiles for equivalence ratio perturbations. (—) is uniform profile, (---) is parabolic profile with side wall fuel injection, and (.....) is with center fuel injection.

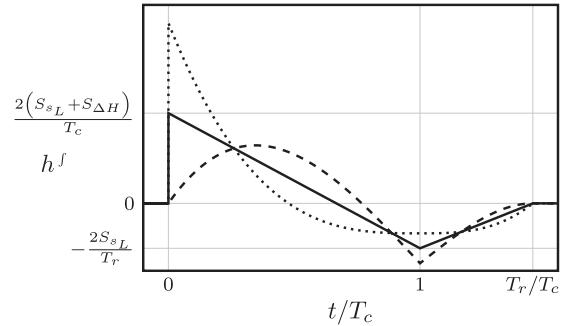


Figure 5. Overall impulse responses for uniform (—), parabolic with side wall fuel injection (---), and with center fuel injection (.....) equivalence ratio perturbations.

dashed and dotted lines correspond to the fuel injection from side walls and the center, respectively. The global time scales, i.e. T_c and T_r , are the same for all perturbations profiles. However, initial response of the side fuel injection is less steep than the uniform profile because the perturbations close to the walls are weak. The positive response region of the parabolic profile is longer. This can be explained by the stronger positive contributions at the center, i.e. the flame speed and heat of reaction contributions, because the equivalence ratio perturbation is higher around the center. This is followed by a narrower but a stronger negative response, which is mainly caused by the flame surface area contribution.

The response of the center fuel injection case is stronger at the beginning compared to the uniform profile due to the large amplitude perturbation close to the walls. However, the positive response region is shorter and followed by a longer and weaker negative response. This is explained by the weak equivalence ratio perturbation close to the center.

The corresponding FTFs are calculated as the Fourier Transform of the IRs. For the case of the uniform perturbation profile, the corresponding results previously derived by Shreekrishna et al.⁹ are recovered

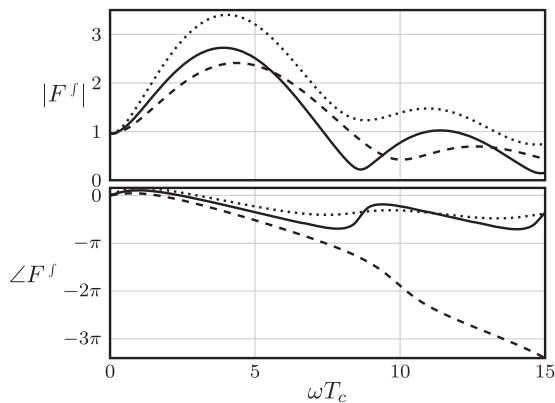


Figure 6. Flame transfer functions for uniform (—), parabolic with side wall fuel injection (---), and with center fuel injection (.....) equivalence ratio perturbations.

exactly. Results are shown in Figure 6. The gain for the case with the side fuel injection is slightly stronger than the other profiles. Considerable deviation is observed in phase for the case with the center fuel injection.

5. Conclusion

The linear response of a technically premixed flame to perturbations of equivalence ratio is investigated using a level set method (“ G -equation”). In particular, the time-domain-based, analytical model proposed by Albayrak et al.¹⁰ is extended to account for local modulations of fuel concentration, which are likely to result from imperfect fuel–air premixing in technical applications. Three major contributions to the fluctuations in heat release rate—related to modulation of heat of reaction, laminar flame speed, and flame surface area, respectively⁸—are analyzed for the case of a local perturbation. It is demonstrated that the heat of reaction and laminar flame speed contributions are local processes in the sense that the flame response is activated once the perturbation reaches the flame. Therefore, they are characterized by a local convective time scale τ_c , which is the time for the local perturbation to travel from the flame base to the flame surface. The third contribution, related to flame surface area, is an indirect mechanism caused by the modulation of the laminar flame speed, which locally induces a wrinkle in the flame shape that propagates towards the flame tip. This process is related to the restoration time scale τ_r , identified by Blumenthal et al.¹¹ Thus, the flame surface area affects the heat release rate during a time interval from τ_c to τ_r .

For validation purposes, the IR to a perturbation with uniform profile, which was already studied by Albayrak et al.¹⁰ and Cho and Lieuwen,⁸ is recovered with the method proposed in this paper. Moreover, the method is applied in an exemplary manner to two

parabolic perturbation profiles, which can be regarded as a technically premixed case with fuel injection from the center and side walls, respectively. It is shown that the flame response, particularly the phase of the FTF, can be altered significantly by the non-uniformity of equivalence ratio perturbations.

The local flame IR is a simple yet powerful concept, which allows to determine the response to arbitrary profiles of equivalence ratio perturbations as an integral over local perturbations. Closed form analytical solutions for the flame impulse can be found if mean equivalence ratio and mean flow velocities are assumed to be uniform, as was the case in the present study. More complicated configurations can be calculated numerically, however the underlying physics is the same. Including the generation and propagation of local equivalence ratio fluctuations in more realistic flow configurations can be an interesting future work. The impact of the local convective time scales on the flame response can be analyzed.

In this work, the time domain approach is preferred over the frequency domain approach, although they contain the same information. This is justified by the convective processes, which can be interpreted from a time domain approach. The local response can be also derived in the frequency domain as the FTF, which can be extended for the case the weakly non-linear response.

Acknowledgments

The presented work is part of the Marie Curie Initial Training Network Thermo-acoustic and aero-acoustic nonlinearities in green combustors with orifice structures (TANGO).

Declaration of Conflicting Interests

The author(s) declared no potential conflicts of interest with respect to the research, authorship, and/or publication of this article.

Funding

The author(s) disclosed receipt of the following financial support for the research, authorship, and/or publication of this article: the European Commission under call FP7-PEOPLE-ITN-2012 and the Research Association for Combustion Engines (Forschungsvereinigung Verbrennung e.V.—FVV, project number: 6011702).

Note

a. Some authors prefer the term “practical premixed flames”.

References

1. Lawn CJ and Polifke W. A Model for the Thermoacoustic Response of a Premixed Swirl Burner, Part II: The Flame Response. *Combust Sci Technol* 2004; 176: 1359–1390.

2. Lieuwen TC. *Unsteady combustor physics*. UK: Cambridge University Press, 2012.
3. Kerstein AR, Ashurst WT and Williams FA. Field Equation for Interface Propagation in an Unsteady Homogeneous Flow Field. *Phys Rev A* 1988; 37: 2728–2731.
4. Boyer L and Quinard J. On the Dynamics of Anchored Flames. *Combust Flame* 1990; 82: 51–65.
5. Fleifil A, Annaswamy AM, Ghoneim ZA, et al. Response of a Laminar Premixed Flame to Flow Oscillations: A Kinematic Model and Thermoacoustic Instability Results. *Combust Flame* 1996; 106: 487–510.
6. Schuller T, Durox D and Candel S. A Unified Model for the Prediction of Laminar Flame Transfer Functions: Comparisons Between Conical and V-Flame Dynamics. *Combust Flame* 2003; 134: 21–34.
7. Dowling AP and Hubbard S. Instability in Lean Premixed Combustors. *Proc IMechE, Part A: J Power and Energy* 2000; 214: 317–332.
8. Cho JH and Lieuwen TC. Laminar Premixed Flame Response to Equivalence Ratio Oscillations. *Combust Flame* 2005; 116–129.
9. Shreekrishna, Hemchandra S and Lieuwen T. Premixed Flame Response to Equivalence Ratio Perturbations. *Combust Theory Modell* 2010; 14: 681–714.
10. Albayrak A, Blumenthal RS, Ulhaq A, et al. An Analytical Model for the Impulse Response of Laminar Premixed Flames to Equivalence Ratio Perturbations. *Proc Combust Inst* 2017; 36: 3725–3732.
11. Blumenthal RS, Subramanian P, Sujith R, et al. Novel Perspectives on the Dynamics of Premixed Flames. *Combust Flame* 2013; 160: 1215–1224.
12. Abu-Off G and Cant R. Reaction Rate Modeling for Premixed Turbulent Methane-air Flames. In: *Proceedings of the joint meeting of Spanish, Portuguese, Swedish and British Sections of the Combustion Institute, Madeira, 1996*.

Appendix I

The derivation of the heat of reaction contribution to the impulse response for the uniform perturbation $h_{\Delta H}^f(t)$ (equation (23)) is demonstrated starting from the local heat of reaction contribution $h_{\Delta H}(a, t)$ (equation (20)).

Substituting equation (20) in the integral in equation (22) yields

$$h_{\Delta H}^f(t) = \frac{2S_{\Delta H}}{R^2} \int_0^R a \delta(t - \tau_c) da \quad (35)$$

where $\tau_c = T_c(1 - a/R)$ is valid for a conical flame. The change of variables $b = t - T_c(1 - a/R)$ yields

$$h_{\Delta H}^f(t) = \frac{2S_{\Delta H}}{T_c^2} \left[\int_{t-\tau_c}^t b \delta(b) db + (T_c - t) \int_{t-\tau_c}^t \delta(b) db \right] \quad (36)$$

The first integral is zero. The second integral is evaluated by using the fact that the Heaviside step function is the anti-derivative of the Dirac delta function. The result reads

$$h_{\Delta H}^f(t) = \frac{2S_{\Delta H}}{T_c^2} (T_c - t) [H(t) - H(t - T_c)] \quad (37)$$

Now, we derive the same for the parabolic profile that corresponds to the center fuel injection case. Substituting the form factor $C_f = 2a^2/R^2$ into equation (32), the integral term reads

$$h_{\Delta H}^f(t) = \frac{2S_{\Delta H}}{R^4} \int_0^R a^3 \delta(t - \tau_c) da \quad (38)$$

Again, we perform the change of variables $b = t - T_c(1 - a/R)$. The resulting integral reads

$$h_{\Delta H}^f(t) = \frac{2S_{\Delta H}}{T_c^4} \int_{t-\tau_c}^t (b - t + T_c)^3 \delta(b) db \quad (39)$$

Since all integrals $\int b^n \delta(b) db$ with $n \in \mathbb{N}_1$, the only the integral with $n=0$ remains

$$h_{\Delta H}^f(t) = \frac{2S_{\Delta H}}{T_c^4} (T_c - t)^3 \int_{t-\tau_c}^t \delta(b) db \quad (40)$$

This integral is calculated as

$$h_{\Delta H}^f(t) = \frac{2S_{\Delta H}}{T_c^4} (T_c - t)^3 [H(t) - H(t - T_c)] \quad (41)$$

The flame surface area contribution is calculated in an analogous manner.